BMC Medical Imaging

RESEARCH

Open Access

Clinical and CT characteristics for predicting lymph node metastasis in patients with synchronous multiple primary lung adenocarcinoma

Yantao Yang[1†], Ziqi Jiang[2†], Qiubo Huang[1†], Wen Jiang[3†], Chen Zhou[1], Jie Zhao[1], Huilian Hu[1], Yaowu Duan[1], Wangcai Li[1], Jia Luo[4], Jiezhi Jiang[5] and Lianhua Ye[1*]

Abstract

Purpose This study aims to investigate the risk factors for lymph node metastasis (LNM) in synchronous multiple primary lung cancer (sMPLC) using clinical and CT features, and to offer guidance for preoperative LNM prediction and lymph node (LN) resection strategy.

Materials and methods A retrospective analysis was conducted on the clinical data and CT features of patients diagnosed with sMPLC at the Third Affiliated Hospital of Kunming Medical University from January 1, 2018 to December 31, 2022. Patients were classified into two groups: the LNM group and the non-LNM (n-LNM) group. The study utilized univariate analysis to examine the disparities in clinical data and CT features between the two groups. Additionally, multivariate analysis was employed to discover the independent risk variables for LNM. The diagnostic efficacy of various parameters was evaluated using the receiver operating characteristic (ROC) curve.

Results Among the 688 patients included in this study, 59 exhibited LNM. Univariate analysis revealed significant differences between the LNM and n-LNM groups in terms of gender, smoking history, CYFRA21-1 level, CEA level, NSE level, lesion type, total lesion diameter, main lesion diameter, spiculation sign, lobulation sign, cavity sign, and pleural traction sign. Logistic regression identified CEA level (OR = 1.042, 95%CI: 1.009-1.075), lesion type (OR = 9.683, 95%CI: 3.485-26.902), and main lesion diameter (OR = 1.677, 95%CI: 1.347-2.089) as independent predictors of LNM. The regression equation for the joint prediction was as follows: logit(p)= -7.569+0.041*CEA level +2.270* lesion type +0.517* main lesion diameter.ROC curve analysis showed that the AUC for CEA level was 0.765 (95% CI, 0.694–0.836), for lesion type was 0.794 (95% CI, 0.751–0.838), for main lesion diameter was 0.830 (95% CI, 0.784–0.875), and for the combine predict model was 0.895 (95% CI, 0.863–0.928).

Conclusion The combination of clinical and imaging features can better predict the status of LNM of sMPLC, and the prediction efficiency is significantly higher than that of each factor alone, and can provide a basis for lymph node management decision.

Keywords Synchronous multiple primary lung cancer, Clinical features, Lymph node metastasis, Risk factor

†Yantao Yang, Ziqi Jiang, Qiubo Huang and Wen Jiang contributed equally to this work.

*Correspondence:
Lianhua Ye
Lhye1204@aliyun.com
Full list of author information is available at the end of the article

Introduction

Based on the 2022 figures provided by the National Cancer Center, lung cancer continues to be the primary cause of illness and death associated to cancer in China [1]. The extensive utilization of low-dose spiral CT has resulted in the heightened identification of small, numerous lung nodules [2]. Studies suggest that multiple nodules often signify Multiple primary lung cancer(MPLC), with sMPLC being a significant subset [3].

Surgical treatment is the primary approach for MPLC. However, the selection of the surgical method remains controversial due to the multiple lesions [4]. Sublobectomy is favored over lobectomy by many scholars for treating MPLC, which frequently presents as ground-glass nodules [5–7].

The multiple lesions make surgeons pay more attention to the lesions themselves during surgery, but the management of lymph nodes was neglected. This may lead to the omission of some lymph nodes with occult metastases. Many studies have shown that lymph node metastasis is an independent risk factor for MPLC prognosis [8–10]. Therefore, it is necessary to evaluate lymph node metastasis in MPLC.

Imaging techniques are increasingly used in clinical diagnosis [11–13]. Previous research has demonstrated that both clinical and imaging features can predict LNM in NSCLC [14–16]. Terumoto Koike et al. [14] indicated that tumor size are predictive of LNM. Keiju et al. [17] demonstrated that tumor diameter is a significant predictor of lymph node metastasis (LNM), a finding consistent with the results reported by other researchers [18, 19]. Moon et al. [20] identified carcinoembryonic antigen (CEA) levels as a risk factor for LNM, a conclusion echoed by Zhou et al. [21]. Additionally, Ye et al. [15] emphasized the pivotal role of nodule type in predicting LNM, a perspective further validated by Chen et al. [22]. Zhang et al. [23] noted that solid nodules exhibit a higher propensity for LNM. Furthermore, Li et al. [24] highlighted the predictive value of CT imaging signs for assessing LNM. Zhou et al. [21] also underscored the vascular convergence sign as a crucial indicator of LNM. Zhang et al. [23] further identified cavitary signs and pleural traction signs as important factors in predicting LNM. Fan et al. [25] demonstrated that combining CT imaging features with serological markers significantly enhances the predictive accuracy for LNM, achieving an area under the curve (AUC) value of 0.916.

However, most of the above studies were based on single lung cancer cases. Due to the unique biological characteristics of MPLC, it has not been reported whether the relevant predictors of lymph node metastasis are similar. Moreover, previous studies mostly focused on the correlation between a single feature and lymph node metastasis. In MPLC, whether the combination of clinical and imaging features can improve the diagnostic efficiency needs to be further verified. Due to the limitations of clinical data on heterochronous multiple primary lung cancer, synchronous multiple primary lung cancer provides us with a relatively large sample study. Based on this, we plan to conduct a large sample study to systematically explore the correlation between clinical and imaging features and lymph node metastasis of sMPLC, and determine independent predictors, so as to provide reference for lymph node resection of synchronous multiple primary lung adenocarcinoma.

Materials and methods

Participants

A retrospective analysis was conducted on the clinical and imaging data of patients with sMPLC, as defined by the 2013 ACCP criteria, who had surgical resections performed at the Third Affiliated Hospital of Kunming Medical University either simultaneously or in stages from January 1, 2018, to December 31, 2022. Kunming Medical University's Third Affiliated Hospital (Yunnan Cancer Hospital) Ethics Committee gave their stamp of approval to this research. The ethics review number is KYLX2024-006. diagnostic criteria: The sMPLC diagnostic criteria of ACCP in 2013 were adopted in this study [26]: (1)anatomically independent locations for each lesion; (2) different histopathological types; (3) for lesions with identical histopathology, requirements were: (a) location in different lung segments, lobes, or sides, originating from distinct in situ cancers; (b) no involvement of a common LN drainage area; (c) absence of distant metastasis; (d) an interval of less than two years between tumor developments. Inclusion criteria were: (1) availability of CT images within two weeks prior to surgery, showing more than two independent lesions; (2) postoperative diagnosis of sMPLC within a two-year interval; (3) absence of distant metastasis; (4) age of 18 years or older. Exclusion criteria included: (1) no LN treatment during surgery; (2) history of other malignancies; (3) preoperative treatments like chemotherapy, radiotherapy, or radiofrequency ablation; (4) artifacts affecting CT image assessment; (5) incomplete clinical data.

CT acquisition

The imaging data of patients undergoing preoperative chest CT examination in our hospital were collected. During chest CT scan, the patient was placed in a supine position with arms raised and breath held after deep inhalation. Set the tube voltage to 120 kV, current to 100 mA, pitch to 1.0, layer thickness to 1 mm, spiral scanning from lung tip to lung base. The scanning parameters are 70 kV, 50mAs, 512×512 matrix. Lung window: Window width 1200HU ~ 1500HU, window position -600HU ~ -700HU.

CT image interpretation

CT signs were analyzed, recorded, and diagnosed by two experienced senior thoracic diagnostic radiologists who were blind to the pathological findings and the patients' clinical data. They used both axial CT images and MPR images for assessment. Following independent evaluations, any discrepancies were resolved by consensus. The CT features are described as follows: (1) Lesion location: The location relationship of each lesion was recorded, including the same lobe, different lung lobes on the same side, and bilateral; (2) Lesion diameter: refer to the 2017 Fleischner Society lung nodule CT measurement method [27]. (3) Lesion type (I) Pure ground glass opacity(PGGO): tumor without a solid component that obscures the underlying lung parenchyma other than blood vessels on thin-slice CT (II) Mixed ground glass opacity(MGGO): tumor with a solid component obscuring the underlying lung parenchyma other than blood vessels on thin-slice CT scan viewed on CT lung window settings(III) Pure solid lesion(PSL). (4) spiculation: Presence of a spinous process or thin, short fibrous band extending from the lesion edge to the lung parenchyma, without significant contact with the pleura [28]. (5) Lobulation: Lesion surface exhibiting multiple uneven arcs, suggestive of nodule fusion [29]. (6) vacuole sign: One or more round or oval translucent shadows under 5 mm within the lesion, with well-defined edges [30]. (7)cavity sign: Necrotic and liquefied central tissue of the lesion, forming a gas-filled space post-discharge through the bronchus [31]. (8) Air-bronchogram sign: Visible air shadows within the lesion, with distorted and dilated bronchial flow [32]. (9) vascular convergence sign: Blood vessels adjacent to the lesion are pulled towards and converge due to lesion growth [33]. (10) Pleura traction sign: Appears as a strip or triangular image connecting the nodule and the pleura [34]. We define the lesion type as follows: If all lesions were GGO, it was defined as PGGO group. Part solid lesions appeared and were classified as MGGO group, while pure solid lesions appeared were classified as PSL group.

Pathological diagnosis

According to the 5th edition of the WHO Thoracic Tumor Classification from 2021 [35, 36], this histological subtypes were assessed using a semi-quantitative method with 5% increments, noting the proportion of each subtype within the lesion. The subtype representing the largest proportion was recorded as the dominant pathological subtype. When high-grade components such as micropapillae and solid types exceeded 5%, these were recorded as the predominant subtype.

Statistical methods

When comparing the LNM and non-LNM groups, continuous variables that followed a normal distribution were tested using two independent sample t-tests. For data that did not follow a normal distribution, the Mann–Whitney U test was employed. We used the Pearson chi-square test to examine the categorical variables. Variables that demonstrated significant differences ($P<0.05$) in the univariate analysis were subjected to binary logistic regression. By using a backward elimination process, a logistic regression model was built. To conduct all statistical analyses, SPSS (version 27.0) was utilized. The maximum Youden's index was used to establish the cut-off value. MedCalc software (version 20.217) was used to create ROC curves. We used area under the curve (AUC) to find out how well each risk factor worked on its own and when combined. Statistical significance was determined when $P<0.05$.

Results

Clinical characteristics

The study included 688 patients(Fig. 1), comprising 454 females (65.99%) and 234 males (34.01%). Of these, 495 patients (71.95%) were under 60 years old, and 193 patients (28.05%) were 60 years or older. There were 542 non-smokers (75.78%) and 146 smokers (21.22%). LNM was observed in 59 patients (8.6%). Table 1 presents detailed clinical data.

Correlations of LNM with clinical features

Two groups were formed: LNM and n-LNM, according to the patients. Univariate analysis showed that gender($p<0.01$), smoking history($p<0.01$), CEA level($p<0.01$), CYFRA21-1 level($p<0.01$) and NSE level($p=0.047$) were correlated with LNM of SMPLC. An independent risk factor for LNM in SMPLC was revealed by multivariate analysis as CEA level (OR, 1.032; 95% CI, 1.002–1.063, $p=0.039$) (Table 2, 4).

Correlation of LNM with CT features

Univariate analysis showed that main lesion diameter ($p<0.01$), sum of the diameters of each lesion ($p<0.01$), lesion type ($p<0.01$), spiculation ($p<0.01$), lobulation ($p<0.01$), cavity sign ($p<0.01$), and pleural traction sign ($p<0.01$) were associated with LNM in SMPLC. Multivariate analysis found that lesion type (OR, 8.603; 95% CI, 3.014–24.557, $p<0.01$) and main lesion diameter (OR, 1.613; 95% CI, 1.052–2.474, $p=0.028$) were independent risk factors for LNM in SMPLC (Table 3, 4). The regression equation for the joint prediction was as follows: logit(p) = -7.569 + 0.041*CEA level + 2.270* lesion type + 0.517* main lesion diameter.

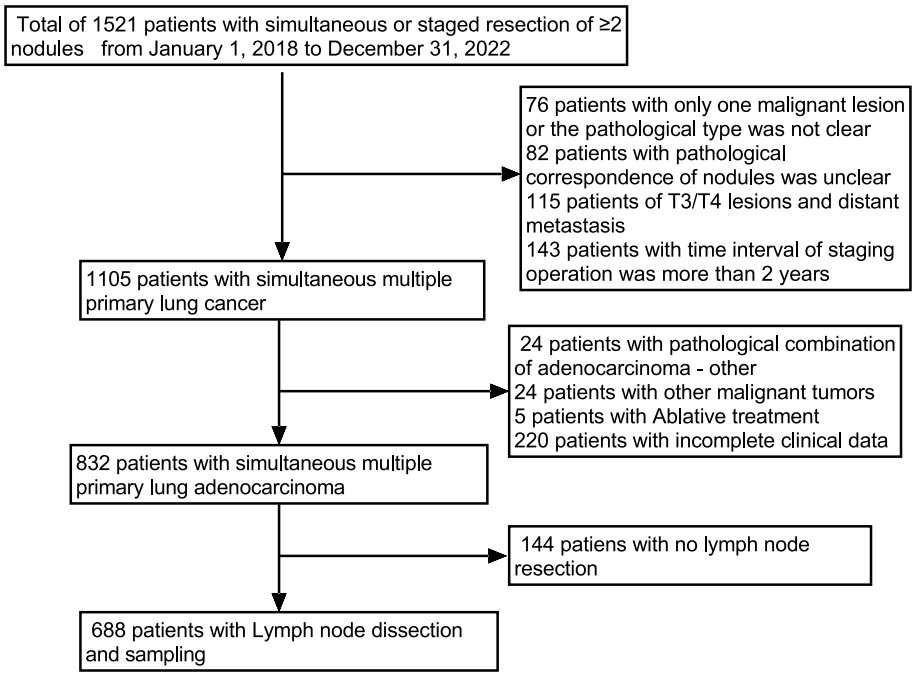

Fig. 1 Patient screening flowchart

ROC curve analysis

The ROC curve, constructed from independent risk factors, indicated that CEA level, lesion type, and main lesion diameter could predict LNM status in SMPLC, with AUC values of 0.765 (95% CI, 0.694–0.836), 0.794 (95% CI, 0.751–0.838), and 0.830 (95% CI, 0.784–0.875), respectively. Combining these three factors, the AUC value reached 0.895 (95% CI, 0.863–0.928), demonstrating enhanced diagnostic capability (Fig. 2, Table 5, 6). The Youden index was used to find that the best cutoff values for CEA level were 4.41 μg/L and for primary lesion diameter were 1.50 cm (Table 5).

Discussion

Lung cancer is one of the most serious malignant tumors in the world, and adenocarcinoma is its most important type [37]. With the implementation of early diagnosis and early treatment of lung cancer, more and more early lung adenocarcinomas manifested as lung nodules have been found, and the proportion of multiple primary lung adenocarcinomas is increasing year by year, and simultaneous multiple primary lung cancer is an important part of it [2, 38, 39].

Previous research [40, 41] has emphasized that surgical treatment is crucial for sMPLC, and LN management is particularly critical. The intraoperative assessment of LNM is often limited. thus, using preoperative data to predict LNM offers distinct advantages. Earlier studies [15, 42–44] have demonstrated that clinical and radiographic features can assess LNM in lung cancer. However, most studies have investigated the relationship between a single feature and LNM on the basis of small sample and typically addressed single lung cancer cases. The correlation between these features and LNM in sMPLC remains uncertain, and whether a combination of clinical and imaging features can enhance diagnostic efficiency is still under investigation. Therefore, we conducted a large-sample study to systematically explore the relationship between clinical and imaging features and lymph node metastasis in sMPLC, and find independent predictors to evaluate the status of lymph node metastasis, providing evidence for the decision of lymph node management in patients with simultaneous multiple primary lung cancer.

Unlike traditional lung cancer, which tends to affect older, smoking males, sMPLC in our study was more prevalent among younger, non-smoking females, likely due to the frequent presentation of ground-glass nodules, which exhibit distinct epidemiological traits. Chen et al. [45] identified age as an independent predictor of LNM in lung cancer, a finding further confirmed by Xue et al. [46]. Our findings are contrary, which may be due to differences in the included samples. Xue et al. [46] noted that gender was not linked to LNM in sMPLC, aligning with our observations.

CEA level is an important factor in evaluating LNM in lung cancer. Ye et al. demonstrated [15] in a study involving 651 patients that CEA level was an independent

Table 1 Baseline data of the patient

Variables	Number	Percentage (%)
Gender		
Female	454	65.99
Male	234	34.01
Age		
< 60	495	71.95
≥ 60	193	28.05
Smoking history		
No	542	78.78
Yes	146	21.22
Family history of cancer		
No	587	85.32
Yes	101	14.68
Xuanwei area		
No	313	45.49
Yes	375	54.51
Mode of operation		
Wedge resection	108	15.7
Segmentectomy	50	7.27
Lobectomy	186	27.03
Lobectomy + Wedge resection	205	29.8
Lobectomy + segmentectomy	38	5.52
Segmentectomy + Wedge resection	90	13.08
Lobectomy + segmentectomy + Wedge resection	11	1.6
Lymph node status		
N0	629	91.42
N1	17	2.47
N2	18	2.62
N1 + N2	24	3.49
Primary lesion pathology		
Adenocarcinoma In Situ	7	1.02
Minimally Invasive Adenocarcinoma	114	16.57
Lepidic Predominant	157	22.82
Acinar predominant	173	25.15
Papillary Predominant	105	15.26
Solid Predominant	31	4.51
Micropapillary Predominnat	79	11.48
Mucinous adenocarcinoma	22	3.2

predictor of LNM, a finding further confirmed by Zheng et al. [42]. The higher the CEA level, the greater the likelihood of LNM. Our results are similar. CEA levels have been shown for the first time to be an independent predictor of lymph node metastasis in sMPLC, and the best diagnostic efficacy was achieved when CEA levels were greater than 4.41. This may be related to more CEA secretion levels at the time of lymph node metastasis.

Table 2 Relationship between clinical features and lymph node metastasis in sMPLC

Variables	n-LNM	LNM	*P*
Age(%)			0.867
< 60	452 (71.86)	43 (72.88)	
≥ 60	177 (28.14)	16 (27.12)	
Gender(%)			0.000**
Female	431 (68.52)	23 (38.98)	
Male	198 (31.48)	36 (61.02)	
Xuanwei area(%)			0.437
No	289 (45.95)	24 (40.68)	
Yes	340 (54.05)	35 (59.32)	
Family history of cancer(%)			0.523
No	535 (85.06)	52 (88.14)	
Yes	94 (14.94)	7 (11.86)	
Smoking history(%)			0.000**
No	506 (80.45)	36 (61.02)	
Yes	123 (19.55)	23 (38.98)	
CEA level (ng/ml)	2.31 (1.50,3.50)	5.34 (2.50,13.30)	0.000**
CYFRA21-1 level (ng/ml)	2.30 (1.80,3.10)	3.20 (2.40,4.10)	0.000**
NSE level(ug/l)	12.60 (11.00,14.60)	13.40 (11.70,15.20)	0.047*
SCC level(ug/l)	0.70 (0.60,1.00)	0.70 (0.60,1.00)	0.551

* $p < 0.05$, ** $p < 0.01$

Tumor diameter is closely related to tumor aggressiveness [47]. The larger the tumor, the more aggressive it is, increasing the likelihood of metastasis. Koike et al. [14] analyzed 894 patients with stage Ia non-small cell lung cancer (NSCLC) and identified a nodule diameter ≥ 2 cm as a predictive factor for mediastinal LNM. Zhang et al. [48] and Fuwa [49] also reported that tumor diameter is an independent risk factor for LNM, with Fuwa noting a 44% metastasis rate in tumors larger than 4.1 cm. In sMPLC, our study uniquely shows that main lesion diameter, particularly when greater than 1.5 cm, independently predicts LNM, with an AUC value of 0.83. Many studies have identified nodule density as a significant predictor of LNM [15, 50]. Koike et al. found [50] that a consolidation tumor ratio (CTR) ≥ 89% was the best predictor of LNM, a result supported by Shao et al. [18] and confirmed in our study. We have also categorized lesion types for the first time and explored their link with LNM in sMPLC. Increased solid components may enhance tumor aggressiveness, potentially driving LNM.

The CT morphological features of lesions, to some extent, reflect nodule aggressiveness. However, assessing LNM status has limitations. Jia et al. [51] showed that spiculation and lobulation signs were not independent risk factors for mediastinal LNM. Other studies indicated that pleural traction, vascular convergence, and cavity

Table 3 Relationship between CT features and lymph node metastasis in sMPLC

Variables	n-LNM	LNM	*P*
Main lesion diameter(cm)	1.40 (1.00,2.00)	3.00 (1.90,4.00)	0.000**
Sum of the diameter of each lesion(cm)	2.50 (1.80,3.50)	4.40 (3.30,5.90)	0.000**
Relative tumor location(%)			0.565
Identical lobe	212 (33.70)	16 (27.12)	
Different lung lobes on the same side	292 (46.42)	31 (52.54)	
bilateral	125 (19.78)	12 (20.34)	
Lesion type(%)			0.000**
GGO	134 (21.30)	0 (0.00)	
MGGO	270 (42.93)	4 (6.78)	
PSL	225 (35.77)	55 (93.22)	
spiculation(%)			0.000**
No	470 (74.72)	26 (44.07)	
Yes	159 (25.28)	33 (55.93)	
lobulation(%)			0.000**
No	463 (73.61)	24 (40.68)	
Yes	166 (26.39)	35 (59.32)	
vacuole sign(%)			0.751
No	457 (72.66)	44 (74.58)	
Yes	172 (27.34)	15 (25.42)	
cavity sign(%)			0.000**
No	612 (97.30)	51 (86.44)	
Yes	17 (2.70)	8 (13.56)	
vascular convergence sign(%)			
No	608 (96.66)	56 (94.92)	0.743
Yes	21 (3.34)	3 (5.08)	
Air Bronchogram Sign(%)			0.971
No	613 (97.46)	51 (86.44)	
Yes	16 (2.54)	8 (13.56)	
Pleura traction sign(%)			0.001**
No	259 (41.18)	11 (18.64)	
Yes	370 (58.82)	48 (81.36)	

* $p < 0.05$, ** $p < 0.01$

signs correlate with LNM but are not independent predictors [51–53]. Similar findings in our study could be attributed to the predominance of early lesions with less pronounced morphological features.

Compared with previous research, our study for the first time systematically analyzed the correlation between clinical and CT features of sMPLC and LNM using a large sample size. Compared to traditional single-feature-based approaches, our study utilized a multi-factorial analysis, incorporating both clinical and CT features, to predict lymph node metastasis in patients with synchronous multiple primary lung cancer (sMPLC). This approach significantly improved diagnostic accuracy. Notably, we were the first to incorporate main lesion diameter and lesion type into a combined predictive model, while also categorizing the lesion types in multiple primary lung cancer. Our combined model achieved an AUC of 0.895, markedly outperforming the predictive power of individual factors.

Table 4 Multivariate analysis of lymph node metastasis

Variables	Odds ratio	Confidence interval	*P*
Gender	1.434	0.594—3.462	0.423
Smoking history	1.115	0.461–2.692	0.809
CEA level	1.032	1.002–1.063	0.039
CYFRA21-1 level	0.985	0.885 -1.095	0.776
NSE level	0.994	0.914 -1.081	0.883
Lesion type	8.603	3.014 -24.557	0.000**
Sum of the diameter of each lesion	1.008	0.728 -1.395	0.964
Main lesion diameter	1.613	1.052- 2.474	0.028
spiculation	1.562	0.798 -3.056	0.193
lobulation	1.087	0.554- 2.133	0.807
cavity sign	1.768	0.576 -5.433	0.319
Pleura traction sign	0.821	0.357 -1.891	0.644

The findings of this study have significant implications for the clinical management of sMPLC. Surgeons can use preoperative prediction models to assess the risk of lymph node metastasis in patients with multiple primary lung adenocarcinomas. If the model indicates high risk, they will prioritize lymph node treatment during surgery. If the risk is low, they may opt to skip lymph node resection, enabling a more minimally invasive procedure and faster patient recovery.

With the advancement of science and technology, an increasing number of emerging technologies have been applied to clinical diagnosis [54–57]. However, due to regional disparities in development, the widespread implementation of these technologies remains limited. As a result, traditional diagnostic methods continue to demonstrate their unique advantages [58, 59]. Our findings indicate that the combined use of clinical and imaging features can achieve favorable results in predicting lymph node metastasis in multiple primary lung adenocarcinoma. This approach offers greater applicability in

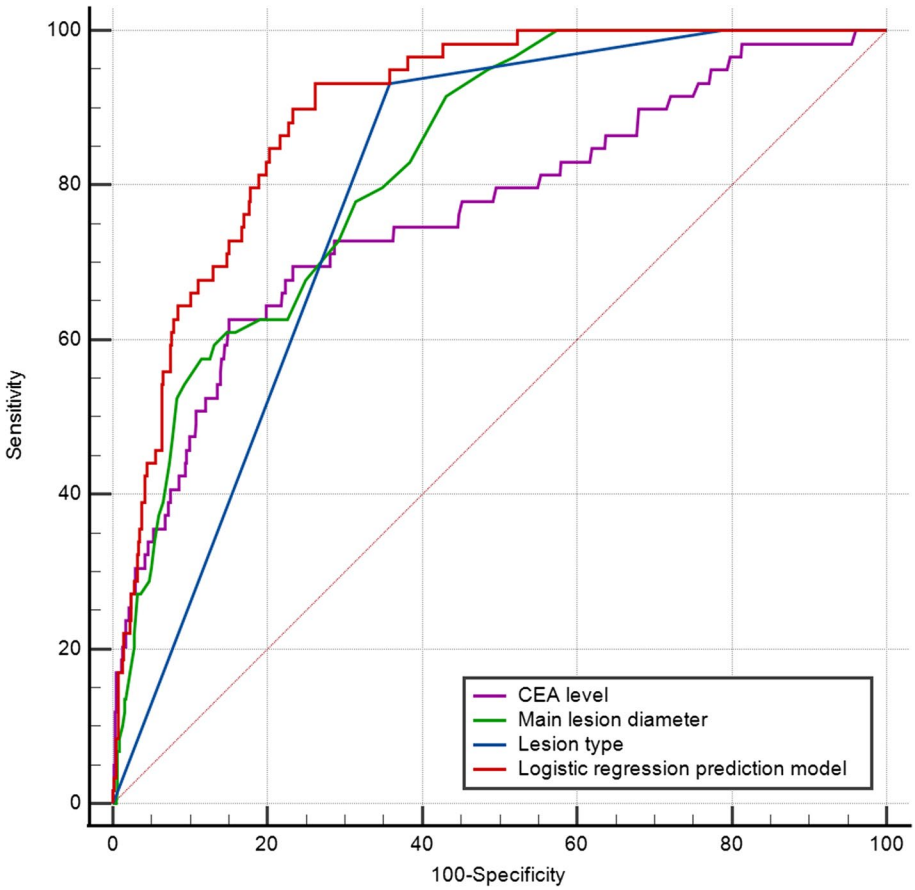

Fig. 2 Summary of ROC Curves

resource-limited settings, making it more conducive to widespread adoption.

In this study, patient data was handled with strict confidentiality, following the guidelines of the Kunming Medical University's Third Affiliated Hospital (Yunnan Cancer Hospital)'s ethics committee. All records were anonymized before analysis to protect patient identities. As the study was retrospective, explicit consent for this research was waived, though general consent for the use of medical records in research was obtained at admission. The use of data adhered to the Declaration of Helsinki's ethical standards, with access limited to authorized personnel for research purposes only. The predictive models were solely for research and not applied in clinical practice. Ongoing ethical oversight ensures responsible use of patient data in future studies.

Despite these promising results, several limitations merit discussion: (1) This study is a single-center retrospective study, lacking sufficient prospective evidence support, There was selective bias in the inclusion of cases. (2) There are subjective errors in the measurement of the image morphological characteristics of nodules, which may cause certain deviations in the results. (3) Despite using clinical and imaging features to predict lymph node metastasis in multiple primary lung adenocarcinoma for the first time, the relatively low incidence of lymph node metastasis limits the number of cases available for effective validation. We plan to further validate our model in future studies with larger cohorts.

Table 5 Summary of ROC curve AUC values

Variables	AUC	Confidence interval	Cutoff value
CEA level	0.765	0.694 -0.836	4.41
Main lesion diameter	0.83	0.784—0.875	1.5
Lesion type	0.794	0.751 -0.838	
Prediction model	0.895	0.863 -0.928	

Table 6 Pairwise comparison of ROC curves

Variables	AUC difference value	Confidence interval	*P*
CEA level-Lesion type	-0.03	-0.108 ~ 0.048	0.457
CEA level-Main lesion diameter	-0.065	-0.152 ~ -0.005	0.08
CEA level-Prediction model	-0.13	-0.225 ~ -0.118	0.000**
Lesion type-Main lesion diameter	-0.035	-0.058 ~ -0.056	0.189
Lesion type-Prediction model	-0.101	-0.120 ~ -0.067	0.000**
Main lesion diameter-Prediction model	-0.066	-0.132 ~ -0.053	0.000**

* $p < 0.05$, ** $p < 0.01$

Conclusion

The combination of clinical and imaging features can better predict the status of LNM of sMPLC, and the prediction efficiency is significantly higher than that of each factor alone, and can provide a basis for lymph node management decision. To enhance the clinical utility of this model, future research could focus on adapting it for other lung cancer subtypes including squamous cell carcinoma and small-cell lung cancer, to determine whether similar predictive efficiencies can be achieved across different histological types. Furthermore, incorporating advanced biomarkers including molecular or genetic markers could further improve the model's accuracy, enabling more personalized and precision-guided treatment strategies for patients.

Acknowledgements
Not applicable.

Authors' contributions
LH Y is responsible for the research topic selection and design, data analysis and interpretation, paper review and revision suggestions; YT Yand ZQ Jand QB H and W J were responsible for the design and implementation of the research topic, data collection, analysis and interpretation, writing the paper, answering the opinions raised and revising the paper. C Z and J Z are responsible for the implementation of the research, the evaluation of the paper and the revision of the paper; YW D and HL H and WC L were responsible for the topic selection and design of the research, data analysis and interpretation, and the review and revision of the opinions of the editorial department. JZ J was responsible for data collection, data analysis and interpretation, and reviewed and revised the opinions of the editorial department. J L is responsible for data collection, data analysis and interpretation, paper review and review of editorial opinions.

Funding
This project was supported by the National Natural Science Foundation of China (82260508), the Yunnan Provincial High-level Health Technical Personnel Training Project (L-2017006), and the Yunnan Provincial Basic Research Project (202201AY070001-135). Kunming Medical University Joint Project of Science and Technology Department of Yunnan Province(202101AY070001-182).

Data availability
The datasets generated and/or analyzed during the current study are not publicly available due sharing data is not included in our research institution review board but are available from the corresponding author on reasonable request.

Declarations

Ethics approval and consent to participate
This study was conducted in accordance with the Declaration of Helsinki. the Ethics Committee of Yunnan Cancer Hospital approved this retrospective study and waived the requirement for informed consent of the participants.

Consent for publication
Not applicable.

Competing interests
The authors declare no competing interests.

Author details
[1]Department of Thoracic and Cardiovascular Surgery, Yunnan Cancer Hospital, the Third Affiliated Hospital of Kunming Medical University, Kunming City, China. [2]Department of Orthopedics and Pain, Third People's Hospital of Honghe Autonomous Prefecture, Gejiu, China. [3]Department of Thoracic Surgery, The First People's Hospital of Yunnan Province, Kunming, China. [4]Department of Pathology, Yunnan Cancer Hospital, The Third Affiliated Hospital of Kunming Medical University, Kunming, China. [5]Department of Radiology, Yunnan Cancer Hospital, The Third Affiliated Hospital of Kunming Medical University, Kunming, China.

Received: 16 August 2024 Accepted: 14 October 2024
Published online: 29 October 2024

References

1. Yuan MW, Wang HH, Duan RF, et al. Analysis on cancer incidence and mortality attributed to human papillomavirus infection in China, 2016. Zhonghua Liu Xing Bing Xue Za Zhi. 2022;43(5):702–8.
2. Shintani Y, Okami J, Ito H, et al. Clinical features and outcomes of patients with stage I multiple primary lung cancers. Cancer Sci. 2021;112(5):1924–35.
3. Chang YL, Wu CT, Lee YC. Surgical treatment of synchronous multiple primary lung cancers: experience of 92 patients. J Thorac Cardiovasc Surg. 2007;134(3):630–7.
4. Zhao J, Shen Z, Huang Y, et al. Evaluation of surgical outcomes and prognostic factors of second primary lung cancer based on a systematic review and meta-analysis. BMC Surg. 2023;23(1):95.
5. Suzuki K, Koike T, Asakawa T, et al. A prospective radiological study of thin-section computed tomography to predict pathological noninvasiveness in peripheral clinical IA lung cancer (Japan Clinical Oncology Group 0201). J Thorac Oncol. 2011;6(4):751–6.
6. Saji H, Okada M, Tsuboi M, et al. Segmentectomy versus lobectomy in small-sized peripheral non-small-cell lung cancer (JCOG0802/WJOG4607L): a multicentre, open-label, phase 3, randomised, controlled, non-inferiority trial. Lancet. 2022;399(10335):1607–17.
7. Suzuki K, Watanabe SI, Wakabayashi M, et al. A single-arm study of sublobar resection for ground-glass opacity dominant peripheral lung cancer. J Thorac Cardiovasc Surg. 2022;163(1):289-301.e2.

8. Shimada Y, Saji H, Otani K, et al. Survival of a surgical series of lung cancer patients with synchronous multiple ground-glass opacities, and the management of their residual lesions. Lung Cancer. 2015;88(2):174–80.
9. Guo H, Mao F, Zhang H, Qiu Y, Shen-Tu Y. Analysis on the prognostic and survival factors of synchronous multiple primary lung cancer. Zhongguo Fei Ai Za Zhi. 2017;20(1):21–7.
10. Peng Y, Wang H, Xie H, et al. Surgical treatment and prognosis for patients with synchronous multiple primary lung adenocarcinomas. Zhongguo Fei Ai Za Zhi. 2017;20(2):107–13.
11. Ullah F, Nadeem M, Abrar M, Amin F, Salam A, Khan S. Enhancing brain tumor segmentation accuracy through scalable federated learning with advanced data privacy and security measures. Mathematics. 2023;11(19):4189.
12. Ullah F, Nadeem M, Abrar M, et al. Brain tumor segmentation from mri images using handcrafted convolutional neural network. Diagnostics. 2023;13(16):2650.
13. Ullah F, Nadeem M, Abrar M. Revolutionizing Brain Tumor Segmentation in MRI with Dynamic Fusion of Handcrafted Features and Global Pathway-based Deep Learning. KSII Trans Internet Inf Syst. 2024;18(1):105–25.
14. Koike T, Koike T, Yamato Y, Yoshiya K, Toyabe S. Predictive risk factors for mediastinal lymph node metastasis in clinical stage IA non-small-cell lung cancer patients. J Thorac Oncol. 2012;7(8):1246–51.
15. Ye B, Cheng M, Li W, et al. Predictive factors for lymph node metastasis in clinical stage IA lung adenocarcinoma. Ann Thorac Surg. 2014;98(1):217–23.
16. Fan XH, Xu XC, Liu XY, et al. Analysis of risk factors for lymph node metastasis in clinical stage T1 lung adenocarcinomas Chin. J Thorac Cardiovasc Surg. 2019;35(07):420–4.
17. Aokage K, Suzuki K, Wakabayashi M, et al. Predicting pathological lymph node status in clinical stage IA peripheral lung adenocarcinoma. Eur J Cardiothorac Surg. 2021;60(1):64–71.
18. Shao W, Zhang Z, Liu Z, et al. The value of pulmonary nodule diameter and consolidation/tumor rate in the prediction of lymph node metastasis in early-stage (cT1N0M0) lung adenocarcinoma. Transl Cancer Res. 2021;10(1):38–46.
19. Jin HY, Xu AH. The value of pulmonary nodule diameter and consolidation to tumor ratio in intraoperative lymph node dissection. J Clin Pulm Med. 2024;29(05):711–7.
20. Moon Y, Choi SY, Park JK, Lee KY. Risk factors for occult lymph node metastasis in peripheral non-small cell lung cancer with invasive component size 3 cm or Less. World J Surg. 2020;44(5):1658–65.
21. Zhou Q, Suzuki K, Anami Y, Oh S, Takamochi K. Clinicopathologic features in resected subcentimeter lung cancer–status of lymph node metastases. Interact Cardiovasc Thorac Surg. 2010;10(1):53–7.
22. Chen YC, Lin YH, Chien HC, et al. Preoperative consolidation-to-tumor ratio is effective in the prediction of lymph node metastasis in patients with pulmonary ground-glass component nodules. Thorac Cancer. 2021;12(8):1203–9.
23. Zhang ZR, Feng HX, Liu Z, et al. Analysis of mediastinal lymph node metastasis of stage cT1a-cN0M0 lung adenocarcinoma. Chin J Clin Thorac Cardiovasc Surg. 2020;27(10):1187–93.
24. Li F, Zhai S, Fu L, Yang L, Mao Y. Nomograms for intraoperative prediction of lymph node metastasis in clinical stage IA lung adenocarcinoma. Cancer Med. 2023;12(13):14360–74.
25. Fan H, Sun P, Wu KW, et al. The predictive value of combining CT with serum CEA, NSE, and Cyfra21-1 for mediastinal lymph node metastasis in non-small cell lung cancer. Shandong Med J. 2022;62(7):57–60.
26. Detterbeck FC, Lewis SZ, Diekemper R, Addrizzo-Harris D, Alberts WM. Executive summary: diagnosis and management of lung cancer, 3rd ed: american college of chest physicians evidence-based clinical practice guidelines. Chest. 2013;143(5 Suppl):7S-37S.
27. Bankier AA, MacMahon H, Goo JM, Rubin GD, Schaefer-Prokop CM, Naidich DP. Recommendations for measuring pulmonary nodules at CT: a statement from the fleischner society. Radiology. 2017;285(2):584–600.
28. Zhang CG. Value of spiculation sign in CT diagnosis of peripheral small lung cancer. J Imaging Res Med Appl. 2020;4(12):124–5.
29. Huang ZB. Lobulation of pulmonary nodules on multi-slice CT and its diagnostic analysis of isolated pulmonary nodules. J Med Jilin. 2014;35(13):2807–8.
30. Zhuang YD, Fu GZ, Ji XW, et al. Correlation of CT features and pathological for pulmonary small nodules with vacuole sign. J Med Imaging. 2019;29(07):1135–40.
31. Ma DQ. Differential diagnosis in pulmonary cavity imaging. Chin. J Radiol. 2004;(01):7-9+14.
32. Huang DP, Fu ZG, Xiang YL, et al. Correlation between abnormal air bronchograms and pathological subtypes in small lung adenocarcinoma with pure ground glass nodule. J Med Imaging. 2019;29(12):2047–50.
33. Liu DY. The diagnostic value of CT reconstruction techniques in the vascular convergence sign of small lung cancer. Clin Pulmonol J. 2014;19(07):1341–3.
34. Qiao PG, Li SS, Zhou J, et al. Multi-planar reconstruction of spiral CT in diagnosis of peripheral pulmonary carcinoma. Chinese J Med Imaging. 2009;17(01):22–4.
35. Nicholson AG, Tsao MS, Beasley MB, et al. The 2021 WHO classification of lung tumors: impact of advances since 2015. J Thorac Oncol. 2022;17(3):362–87.
36. Travis WD, Brambilla E, Noguchi M, et al. International association for the study of lung cancer/american thoracic society/european respiratory society international multidisciplinary classification of lung adenocarcinoma. J Thorac Oncol. 2011;6(2):244–85.
37. Siegel RL, Miller KD, Wagle NS, et al. Cancer statistics, 2023. CA Cancer J Clin. 2023;73(1):17–48.
38. Sadate A, Occean BV, Beregi JP, et al. Systematic review and meta-analysis on the impact of lung cancer screening by low-dose computed tomography. Eur J Cancer. 2020;134:107–14.
39. Niu N, Zhou L, Zhao J, Ma X, Yang F, Qi W. Sublobar resection versus lobectomy in the treatment of synchronous multiple primary lung cancer. World J Surg Oncol. 2023;21(1):135.
40. Tie H, Luo J, Shi R, Li Z, Chen D, Wu Q. Characteristics and prognosis of synchronous multiple primary lung cancer after surgical treatment: A systematic review and meta-analysis of current evidence. Cancer Med. 2021;10(2):507–20.
41. Nie Y, Wang X, Yang F, Zhou Z, Wang J, Chen K. Surgical prognosis of synchronous multiple primary lung cancer: systematic review and meta-analysis. Clin Lung Cancer. 2021;22(4):341-350.e3.
42. Zheng Y, Ju S, Huang R, Zhao J. Lymph node metastasis risk factors in clinical stage IA3 lung adenocarcinoma. J Cancer Res Ther. 2023;19(1):34–8.
43. Fang C, Xiang Y, Han W. Preoperative risk factors of lymph node metastasis in clinical N0 lung adenocarcinoma of 3 cm or less in diameter. BMC Surg. 2022;22(1):153.
44. Wang Y, Jing L, Wang G. Risk factors for lymph node metastasis and surgical methods in patients with early-stage peripheral lung adenocarcinoma presenting as ground glass opacity. J Cardiothorac Surg. 2020;15(1):121.
45. Chen B, Wang X, Yu X, et al. Lymph node metastasis in Chinese patients with clinical T1 non-small cell lung cancer: a multicenter real-world observational study. Thorac Cancer. 2019;10(3):533–42.
46. Xue X, Zang X, Liu Y, et al. Independent risk factors for lymph node metastasis in 2623 patients with Non-Small cell lung cancer. Surg Oncol. 2020;34:256–60.
47. Chu ZG, Li WJ, Fu BJ, Lv FJ. CT characteristics for predicting invasiveness in pulmonary pure ground-glass nodules. AJR Am J Roentgenol. 2020;215(2):351–8.
48. Zhang XF, Jin RS, Zheng YS, et al. Analysis of risk factors for lymph node metastasis in T2 stage non-small cell lung cancer. Chin J Clin Thorac Cardiovasc Surg. 2020;27(10):1194–200.
49. Fuwa N, Mitsudomi T, Daimon T, et al. Factors involved in lymph node metastasis in clinical stage I non-small cell lung cancer–from studies of 604 surgical cases. Lung Cancer. 2007;57(3):311–6.
50. Nakahashi K, Tsunooka N, Hirayama K, et al. Preoperative predictors of lymph node metastasis in clinical T1 adenocarcinoma. J Thorac Dis. 2020;12(5):2352–60.
51. Jia LN, Jia SL, Shen DP. Establishment of CT imaging logistic regression model for mediastinal lymph node metastasis of lung adenocarcinoma and its clinical predictive value. J Med Res. 2022;51(03):48–52.
52. Zhang Y, Shen Y, Qiang JW, Ye JD, Zhang J, Zhao RY. HRCT features distinguishing pre-invasive from invasive pulmonary adenocarcinomas appearing as ground-glass nodules. Eur Radiol. 2016;26(9):2921–8.
53. Peng Xi, Lihui Fu, Huang P. Relationship between CT signs and differentiation degree and lymph node metastasis of ground-glass nodular multifocal Lung Adenocarcinoma. Hebei Med. 2022;28(03):407–12.

54. Bakkouri I, Bakkouri S. 2MGAS-Net: multi-level multi-scale gated attentional squeezed network for polyp segmentation. SIViP. 2024;18(6):5377–86.
55. Bakkouri I, Afdel K. DermoNet: A computer-aided diagnosis system for dermoscopic disease recognition[C]. Image and Signal Processing: 9th International Conference, ICISP 2020, Marrakesh, Morocco, June 4–6, 2020, Proceedings 9. Springer International Publishing; 2020. p. 170–7.
56. Anwar RW, Abrar M, Ullah F. Transfer learning in brain tumor classification: challenges, opportunities, and future prospects. Int Conf Inform Commun Technol Convergence (ICTC). 2023;11:24–9.
57. Ullah F, Nadeem M, Abrar M, et al. Evolutionary model for brain cancer-grading and classification. IEEE Access. 2023;11:126182–94.
58. Yang Y, Xu J, Wang W, et al. A nomogram based on the quantitative and qualitative features of CT imaging for the prediction of the invasiveness of ground glass nodules in lung adenocarcinoma. BMC Cancer. 2024;24(1):438.
59. Yang Y, Zhang L, Wang H, et al. Development and validation of a risk prediction model for invasiveness of pure ground-glass nodules based on a systematic review and meta-analysis. BMC Med Imaging. 2024;24(1):149.

Publisher's Note